International Journal of Aviation, Aeronautics, and Aerospace

Volume 9 | Issue 3 Article 5

2022

Space Harpoon Projectile Analysis for Space Debris Capture

Miraj D. Lathia
University of Nottingham, mirajlathia2@gmail.com
Sam M. Dakka Dr
The University of Nottingham, sam.dakka@tutanota.com

Space Harpoon Projectile Analysis for Space Debris Capture

Cover Page Footnote

The research was conducted in the frame work of Miraj Lathia MEng degree in Aerospace engineering at the University of Nottingham. The research conducted received no funding.

Space debris first began to accumulate in Earth's orbit through the first launch of the artificial satellite Sputnik 1, in October 1957 (NASA, n.d.). Since then, there has been a growing number of derelict objects which are increasing the chances of potential catastrophes including inducing the knock-on effect of space debris, known as the Kessler Syndrome (National Space Centre, 2021). This effect could eliminate Earth's satellite infrastructure, including weather monitoring, navigation and communication which is relied upon by civilization daily. By, 2020, 114 launches carried approximately 1,300 satellites into space, whilst in 2021, this number grew to 1,400 new satellites launched ("How Many," 2021). Predominantly, space debris lies in Low Earth Orbit (LEO), which is within 2,000 km of Earth's surface, although some debris can be found in Geostationary orbit (GEO) which is 35,786 km above the Equator. More than 15,000 pieces of space debris larger than 0.1m across was tracked by the United States Space Surveillance Network (USSSN) in 2021. The altitude determines the time taken for the satellite or debris to return to Earth. Objects below 600 km orbit for several years before re-entering Earth's atmosphere whereas objects above 1,000 km will orbit for centuries (Britannica, n.d.).

Figure 1

Yearly Number of Catalogued Objects in Earth Orbit by Object Type (ARES, n.d.)

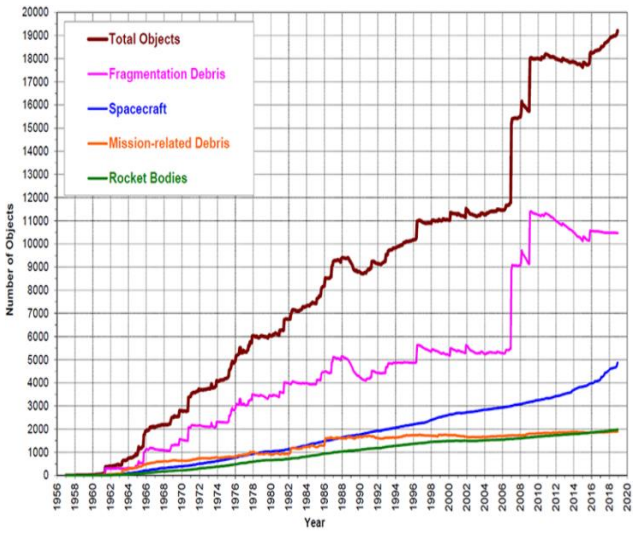

The above graph illustrates the summary of all objects in Earth's orbit, showing a generally steady increase of total objects year on year. Mitigating this growth is essential for a sustainable future within the space market.

To reduce the amount of space debris in orbit, space debris removal systems need to be deployed which fall into either Passive Debris Removal (PDR) or Active Debris Removal (ADR). The space industry tends to focus on the latter with varied technologies. For example, Laser-based systems can be used where a plasma and exhaust plume are created, impacting space debris traveling at high velocities with the intention to make them re-enters the atmosphere. Although, a highly accurate target detection system is needed (Shen et al., 2014). A sail-based system has been tested in industry, where a deployment mechanism extends via a telescopic mast then a drag sail between 16 and 25 square meters is deployed. Surrey Space Centre has tested its sail-based ADR and has concluded that its system can be scaled for use with satellites in

LEO with a size of between 10kg and 1000kg (University of Surrey, n.d.). Nevertheless, the disadvantage of sail-based methods is that it does not pinpoint each intended satellite; a pool of satellites with some unwanted objects might be collected.

A review of the current Technology Readiness Levels or TRLs (Mark & Kamath, 2019) of the most prominent ADRs in the market, with Tether-based and Dynamic systems-based methods showing the highest TRL at an aggregate score of two. Tether-based systems have shown promise for space debris removal, targeting each individual satellite in an accurate manner. The tether is attached to a harpoon head that punctures the target and grapples the satellite back to the space vehicle used to fire the tether. The harpoon heads are the focus of this paper.

LITERATURE REVIEW

Two main designs have been considered for the projectiles. This is the flat head and the conical head. These designs were chosen based on there being more research done on these two shapes than the rest. So, gaining data close to these results would prove a valid experiment. To justify the designs, a ballistic limit velocity must be attained. This velocity is defined as the minimum velocity required to perforate the target plate via the harpoon projectile. The target plate being a one-sided panel, usually made up of a type of Aluminum, which mimics the size and material of typical CubeSats. Attaining a minimal ballistic limit velocity for this experiment is considered the primary target, as a lower ballistic limit caters to a lower propellant requirement, boasting cost and weight-saving elements. Another key element is the fragmentation of the target plates, after the plate has been perforated. Since the aim is to control and mitigate any further space debris creation, minimizing the fragmentation/shattering of the satellite is considered vital. As well as monitoring any debris that has been created from the firing of the projectiles, the perforation profiles of the target plates should be analyzed. The nature of the perforations indicates the tensile stresses associated with each projectile, and thus stresses can be reduced, leading to lower fragmentation, if any.

The Japanese Aerospace Exploration Agency (JAXA) has conducted a similar experiment in which they used multiple harpoon projectiles, with different geometrical profiles, including conical and flat head projectiles (Mataki et al., 2016). After their experiment, the ballistic limit velocity sought for the flat head and conical head were 71.0 m/s and 67.3 m/s respectively. The specifications of the target plate were 200mm x 200mm x 3mm with a mass of 0.32kg. Specifications of both projectiles had a diameter of 0.02m and lengths of 0.1m (Mataki et al., 2016).

The perforation created by the flat projectile shows (Mataki et al., 2016) that material from the plate had to be removed, by punching the plate from the inside out. In contrast, the conical projectile evokes a petaling-like nature where spalling is apparent, and a jagged arrangement is produced compared with the smooth profile of the flat head. These perforation profiles, against the shape of the projectiles, are considered when undertaking the experiment at the University of Nottingham; noting to attain results that are similar. Airbus Defence & Space had also conducted a similar experiment using similar projectile profiles. The length of their flat head was 0.11m and 0.18m for their conical head. The diameter of both their conical and flat heads was 0.016m. The ballistic limit velocity for their flat head and conical head were 33.3-35.5 m/s and 42.9-44.2 m/s respectively (Dudziak et al., 2015). At this point, it is shown that JAXA has a lower ballistic velocity for the conical head, whilst Airbus has a lower ballistic velocity for the flat head. So, the results could seem inconsistent with the

different projectile profiles. Although, it is worth noticing that the length of Airbus' flat head is considerably less than that of their conical head. This could indicate a significant reduction in mass, and therefore a much lower velocity required for penetration. JAXA has the same dimensions for both their flat and conical head and has a lower ballistic limit velocity by 3.7m/s, for the conical head. The difference could also be due to a weight factor because in this case, it should be assumed there is a weight reduction of the conical head due to the angular nature of the lengths mentioned by JAXA, both conical and flat head, are from tip to tip.

EXPERIMENTAL METHOD

The experiment was conducted by using an impact testing laboratory, which consisted of a gas gun chamber, powered by a nitrogen propellant.

Figure 2

Gas Gun Chamber with an Oscilloscope and Impact Area

The gas gun has a length of 4.2m, starting from the point where nitrogen gas is filled (the firing point) through to the nozzle. The nozzle is located within the impact area, located at upper left side in Figure 2, where the aluminum target plates were fixated. The impact area contains a bag of Kevlar at the back of the box, used to absorb any of the impacts from the projectiles that penetrate the aluminum (Al) plates all the way through. The Kevlar was situated 0.73m from the target plate, where the target plate was centered 0.175m from the nozzle. All the events that occurred in the impact area are encompassed within a polycarbonate glass surrounding, for safety measures. The first step in attaining results from the experiment is to have the associated equipment set up prior to any firing. A high-speed camera and corresponding laptop were used to capture the fast-motion impact, and the data given from the camera was used to calculate velocities. To refrain from dull visuals from the camera, 2 Light Emitting Diodes-LED were propped in certain angles so that the images captured were reflected well. To enhance this, an aluminum plate was fixed parallel to the LED lights to reflect light onto the impact area clearly. Figure 3 portrays the impact area seen by the camera, with the 2 LED lights on. A meter rule has been placed within the box to act as a reference placeholder.

Figure 3
Visual of Clamps Holding 1mm Aluminum Plate in Impact Area and Potruding Nozzle of Gas Gun - Seen from Phantom High-Speed Camera

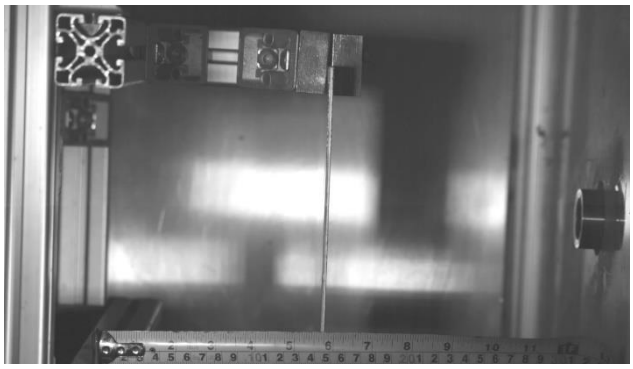

Figure 3 also shows how the aluminum target plates were fixated perpendicular to the nozzle plane. Four (4) bolts on each of the upper and lower clamps prove to suffice when firing projectiles at the higher velocities of the experiment. The other equipment needed to be set up is the oscilloscope, seen in Figure 2. The oscilloscope is used as a verification method, to give justification of the results calculated from the high-speed camera. The oscilloscope is connected to 2 light gates, that are 0.185m away from each other. The 2 lasers shine through small holes within the gas gun chamber and are received by the 2 corresponding light gate sensors. The sensors that are connected to the oscilloscope provide the time difference between when the projectile first interacts with the first light gate, and when it then first interacts with the second light gate. The constant, known distance of 0.185m divided by the different times, is what determines the velocity of the projectiles exiting the nozzle. Once all the equipment is set up, the projectile can be inserted into the chamber, and fired with nitrogen propellant. The pressure that is set, is determined by manually turning a knob, so that a mechanical gauge indicates that the desired pressure in bars has been met. Once the pressure is set, and all safety doors are closed to provide a closed circuit, the capture button is pressed on the laptop. The camera is now ready for an event to take place. Then the trigger for the gas gun is fired and the projectile is propelled towards the target plate. The camera functions at a resolution of 1280 x 800, at 6273 frames per second (fps). The playback of the event also shows the event occurring, frame by frame. Using both of these components, the velocities can be calculated.

The method for testing each harpoon head on cooler Al-aluminum plates, started by submerging the plates within a bag of dry ice. The plates were submerged for 30 minutes before being taken out and clamped in the impact area. The setup was reconfigured as aforementioned and just before the trigger of the camera and gas gun, the temperature of the plate was noted using an infrared thermometer. (*It is worth noting, the time taken between removing the cool plate from the bag and pressing fire for the projectile, takes time and so the plate warms up in room temperature).* The experiment is repeated, for three different pressures, namely, 10, 12.5, and 15 bar, for each of the three different thicknesses of aluminum plates of 1mm,1.5mm, and 3mm, for each of the flat and conical head projectiles and for the cooled plates scenario. A total of 27 firings took place. Only one of each projectile profile was used, as the

geometry of the harpoon heads, even after impact, had not changed. A few scratches were present but no dents or deformations. This meant the designed projectiles proved to be re-usable. The experiment was repeated seamlessly and reliably in the manner aforementioned.

SPECIFICATIONS OF TARGET PLATES AND HARPOON PROJECTILES

Table 1
Material Properties for Tested Al Plates – 1050A (Smith Metal, 2020a)

Tensile Strength (Mpa)	100-135
Yield Strength (Mpa)	Min.75 (approx.)
Shear Strength (Mpa)	70
Elongation (% (A50))	4-8
Brinell Hardness (HB)	35
Thermal Conductivity (W/m.k)	229
Melting Range (K)	918.15 - 930.15
Electrical Conductivity (% IACS)	58.4
Coefficient of Thermal Expansion (1/K)	$23.5x10^{-6}$
Elastic Modulus (Mpa)	69000

Table 1 and Table 2 represent the physical and mechanical properties that the aluminum plates (3mm, 1.5mm, and 1mm) and both conical and flat head projectiles possess. Aluminum was used for the plates in this experiment, as well as comparative literature experiments. Namely, JAXA using A2024-T3 200mm x 200mm x 3mm plates (Mataki et al., 2016) and Airbus using 3mm thick, 5005 Al plates. Comparing the tensile and yield strengths for 3mm thickness plates, Uni of Nottingham's Aluminum 1050A's had the lowest in each compared with JAXAs at 420Mpa and 287Mpa (Smith Meatl, 2020b) and Airbus' at 150Mpa and 193Mpa; for tensile and yield strength respectively (Aalco Metals, 2020; MatWeb, n.d.a). These strengths directly correlate with the residual velocities and the perforation profiles which are analyzed in *later*. Whilst Airbus had not stated the material used for the projectiles, JAXA used S45C Carbon Steel (Mataki et al., 2016).

Table 2
Material Properties for Tested Aluminum Harpoon Projectiles – 6082 (Smith Metal, 2020c)

Tensile Strength (Mpa)	260
Proof Stress (Mpa)	170
Shear Strength (Mpa)	170
Elongation (% (A50))	19
Brinell Vickers (HV)	75
Thermal Conductivity (W/m.k)	180
Melting Point (K)	828.15
Density (kg/m^3)	2700
Coefficient of Thermal Expansion (1/K)	$24x10^{-6}$
Elastic Modulus (Mpa)	70000

which has a higher tensile strength of 686Mpa (MatWeb, n.d.b) compared with the Aluminum 6082 used at Uni Nottingham. The dimensions for the flat head projectile were a simple 20mm diameter x 100mm length, the conical head had a total length of 80mm and had the same bottom diameter of 20mm.

Table 3
Masses (kg) of 3mm, 1.5mm, 1mm Al plates and of Flat and Conical Harpoon Heads

3mm	1.5mm	1mm	Flat Head	Conical Head
0.320	0.165	0.100	0.08075	0.0492

Figure 4
3D Drawing Geometry of Top Part for the Conical Head Projectile

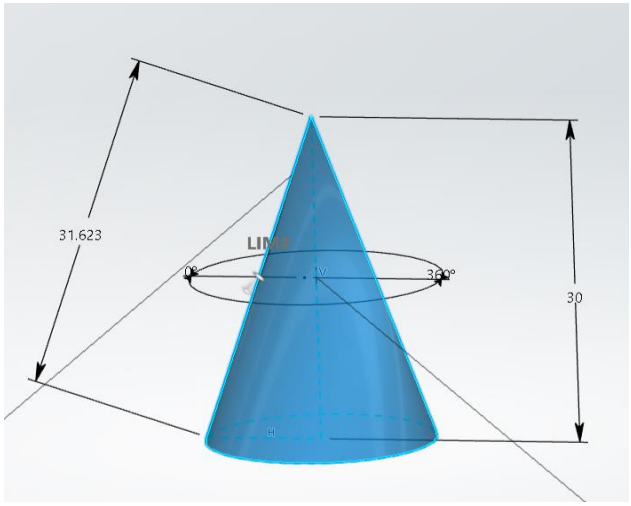

The length of the tip was 30mm as illustrated in Figure 4 whilst the length of the angled side of the tip was 31.623mm. Taking a right-angled triangle template from the bottom of the tip to the top and knowing the mid-point of the tip is 10mm from the edge of the diameter, the angle of the tip can be found to be at 18.44°.

RESULTS & DISCUSSION

The primary objective was to find the Minimum Ballistic Velocity-MBV needed to perforate the plate. The lower the limit, the more efficient the design of the projectile. A ballistic velocity profile is needed to determine the minimum velocity, which can be deduced together from the impact and residual velocity. The impact velocity was calculated by noting the time taken for the projectile to exit the nozzle and touch the front side of the target plate (front side is the side facing the nozzle). This was calculated through the high-speed camera using this calculation:

$$\frac{No.of\ Frames\ from\ Nozzle\ to\ Plate}{Frame\ Rate\ of\ Camera} = Time\ of\ Impact \quad (1)$$

Then, the impact velocity is calculated through this time:

$$\frac{Distance\ between\ Nozzle\ to\ Plate}{Time\ of\ Impact} = Impact\ Velocity \quad (2)$$

The number of frames was calculated through the high-speed camera data, and the frame rate was set at 6273 fps-frames per seconds. The distance between the nozzle and target plate is known at 0.175m.

The residual velocity is the velocity of the projectile when exiting the rear of the plate, after perforation. This was calculated in two ways. The first:

$$\frac{No.of\ Frames\ from\ perforation\ to\ Bag}{Frame\ Rate\ of\ Camera} = Time\ post\ Impact \quad (3)$$

$$\frac{Distance\ between\ Plate\ to\ Bag}{Time\ post\ Impact} = Residual\ Velocity \quad (4)$$

The bag is what absorbs the impact of the projectile, made of Kevlar, and locates 0.73m away from the target plate.

The second method is for scenarios where the projectile does not have enough velocity for it to reach the bag but does have enough to perforate and fall on the rear side of the plate. In this case, the number of frames from the point the leading edge of the projectile perforates the plate, to the point where the trailing edge just leaves the rear of the plate, is noted. This scenario is denoted as LETE (leading edge, trailing edge). The calculation of the residual velocity in this case is:

$$\frac{No.of\ Frames\ of\ LETE}{Frame\ Rate\ of\ Camera} = Time\ of\ LETE \quad (5)$$

$$\frac{L\ of\ Projectile + Thickness\ of\ Plate}{Time\ of\ LETE} = Residual\ Velcocity \quad (6)$$

Figure 5

Ballistic Limit Profiles of Flat and Conical Head Harpoons, against 3mm, 1.5mm, and 1mm Al plates

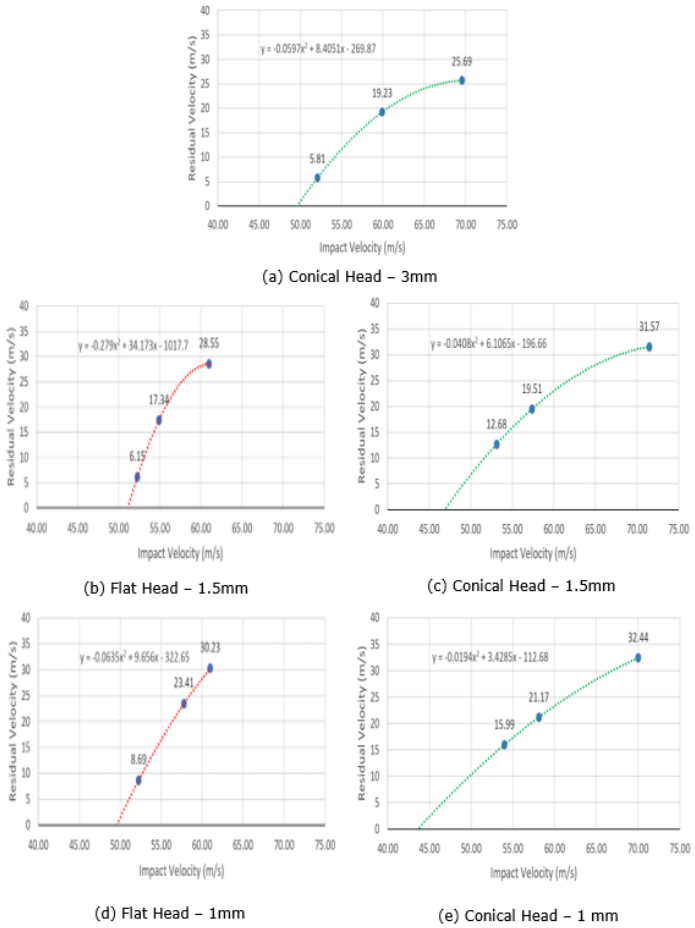

The new distance here is the length (L) of the projectile plus the thickness of the plate. There were scenarios where the projectile would fall in front of the plate, but these situations did not perforate the plate, therefore have not been included in calculations to acquire the ballistic limit velocities.

The two velocities were obtained for both the conical and flat head projectiles, for the three different plate thicknesses, at the three different pressures of 10, 12.5, and 15 bar and then plotted on graphs as shown in Figure 5. The flat head projectiles had not perforated the 3mm plates for all pressures, so a graph has not been presented for this case. The most rightward point of the curves in the graphs of *Figure 5* are projectiles fired at 15 bars, the middle point at 12.5 bar and the most leftward point at 10 bars. The MBV is acquired by the trend line meeting the x-intercept, for each graph. Since it is a quadratic curve, with its respective equation shown within each graph, the 'x' value can be obtained through the Quadratic Formula. This is the MBV. Two 'x' values are found through the formula, though the one of interest is the one illustrated in the graph at the x-intercept.

Table 4

Minimum Ballistic Velocities (m/s) for Flat and Conical Head Projectiles against 3mm, 1.5mm, and 1mm Al plates

	Flat Head	**Conical Head**
3mm	N/A	49.54
1.5mm	51.10	46.90
1mm	49.58	43.64

Table 4 shows that the conical head is superior when looking at attaining the minimum velocity to perforate, with a difference of 5.94 m/s compared with the same plate for the flat head projectile. Against the 3mm plate the conical head has an MBV of 49.54m/s, whilst JAXA has an MBV of 67.3m/s (Mataki et al., 2016). The former being much lower. Even though the diameter of both conical heads is the same, the length and the material used for the harpoon head (therefore the weight) is considerably lower with a difference of 0.2708kg. This shows the substantial effect that mass has on attaining a low MBV. Against the 3mm plate, Airbus had an MBV of 42.9 – 44.2 m/s, for their conical head. The result is very similar to this experiment, and their conical projectile had a slightly smaller diameter and length, inferring a slightly lower mass. The closeness of the results expresses the strong reliability of the experiment. A strong positive correlation can be determined between the increase in plate thickness and the increase in the gradient of the ballistic curves, suggesting the larger the plate thickness the more the residual velocity is affected. Graphs (a) and (c) portray this comparison clearly, with a more curved envelope with (a) than (c). Comparing the profiles between the flat and conical heads, the envelopes of the conical heads are longer than that of the flat, taking (d) and (e) as an example. Both the longer envelopes and larger differences of MBVs between each plate for the conical compared with the flat head, indicate that conical head profiles are more sensitive to the thickness of the plate than flat heads. The sharp tip promotes a

penetration advantage over the flat head as seen by collecting perforation data for 3mm with conical, but no data collated for the flat head at this thickness.

Kinetic energies of the impact and residual velocities can be calculated through the Kinetic Energy equation:

$$\frac{1}{2} * m * V^2 = KE\ (Kinetic\ Energy)\ (7)$$

Figure 6

Energy Differences Against Impact Velocity for Conical and Flat Head Projectiles against 3mm, 1.5mm, and 1mm Al plates

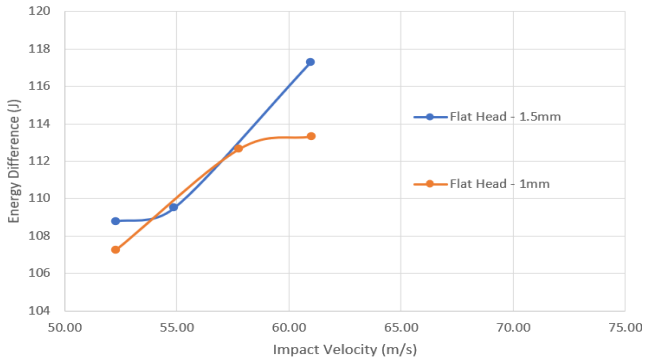

(a) Flat Heads – 1.5mm, 1mm

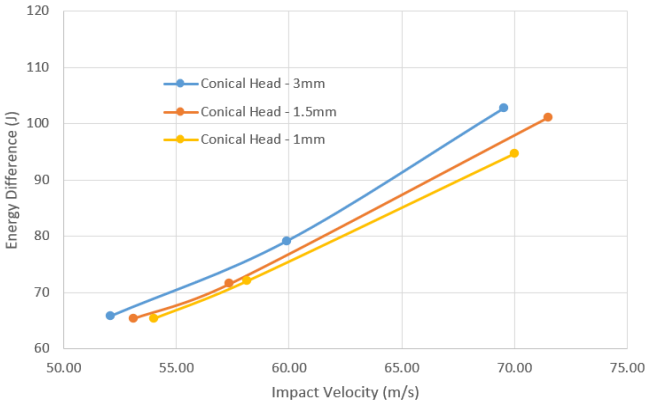

(b) Conical Heads– 3mm, 1.5mm, 1mm

Using the respective masses and velocities for each scenario, the difference in the kinetic energies were calculated by subtracting the absorbed energy (residual) from the impact energy. This plotted against the impact energy gives graphs (a) and (b) in *Figure 6*. Plot (b) shows consistency between the three plates, where the energy difference increases as the impact velocity increases. The gradient becomes steeper from 12.5 to 15 bar compared with 10 to 15 bar. This is also true for plot (a) though specifically for 1.5mm. An anomaly is present with the flat head, 1mm scenario, where

the 12.5 bar firing shows to have a higher impact velocity than what the trends forecast. This could be caused by human error, by setting the pressure to higher than 12.5 bar. When looking at the differences in impact velocity points within Figure 5, its clear to see that each plot has a small difference between 10 and 12.5 bar than it does between 12.5 and 15 bar, apart from (d) – flat head, 1mm. The difference of impact velocities is smaller between 12.5 and 15 bar than that of 10 and 12.5 bar. This reflects clearly in plot (a) of *Figure 6*. The anomaly explicitly portrays the sensitive relationship between the difference in energies against the impact velocity where the higher the impact velocity the higher energy difference.

Cooled Plates-To mimic space-like environments and to analyse the effects of changing material properties of the Al plates, the plates were cooled with dry ice to a temperature of 194.65K (-78.5°C) – captured by an infrared thermometer. The time taken between placing the plate in the clamp, loading the gas and firing the projectile was timed at an average of 90s. Before the trigger was pressed, a new reading of the temperature of the plate was taken, averaging 241.15K (-32°C). The ballistic limit velocity profiles for the cooled plates mirrored the envelope of curves as the ones at room temperature. The noticeable difference was the increase in MBV for both the conical and flat heads with cooled plates. All 3mm flat heads and 10 bar 1.5mm flat head firing did not perforate. *Table 5* breaks down the MBVs for the cooled plates at different bars for each harpoon head. The increase in MBV for cooler temperatures of Al plates can be correlated to the increased yield and tensile strength that Aluminium alloys experience when below 273.15K temperatures (Roth et al., 2020). The increase in strengths of the plates will result in increased MBVs and the reason behind the firing for the flat harpoon at 10 bar against 1.5mm did not perforate.

Table 5

Minimum Ballistic Velocities (m/s) for Flat and Conical Head Projectiles against 3mm, 1.5mm, and 1mm Al plates cooled to approx. 241.15K

	Flat Head	Conical Head
3mm	N/A	53.64
1.5mm	N/A	48.89
1mm	53.03	46.33

Figure 7
Phantom High-Speed Camera visual of Flat Head Projectiles at 10 bar against 1.5mm plates – Cooled and Room Temperature

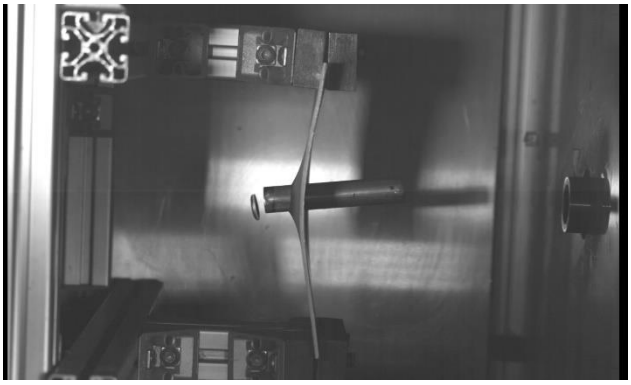

(a) Room Temperature

(b) Cooled to 241.15K

Figure 7 illustrates how the harpoon head punches a hole out of the plate in the room temperature environment, where the cooled plate obstructed the harpoon from continuing its motion. Due to the increase in brittleness and decrease in ductility when cooling has occurred, the perforations aesthetics are contrasted.

Figure 8
Perforation of Flat Head Harpoons against 1mm Plates at 12.5 Bar at Room and Cooled Plate Temperatures

(a) Room Temperature (b) Cooled

Figure 9
Perforation of Conical Head Harpoon against 3mm Plate at 12.5 Bar – Room Temperature

A jagged, rough edge with ridges within the circular hole is present when analyzing image (a) of Figure 8, whilst in contrast, a clean, complete circular hole with no crests is exhibited in image (b). The difference in failure modes can be seen between images in Figure 8 and Figure 9. The 'punching' out effect created by the flat head harpoon is a result of shear failures that are created along the boundary line of the surface of impact (Roth et al., 2020). Whilst the perforation profiles produced by conical heads results in piercing, petaling, and crack propagation (Kpenyigba et al., 2015). Akin to the perforations in Figure 8, are shown in Airbus' report (Dudziak et al., 2015), showing the validity of the results obtained.

The material properties change as the temperature of the material changes, conducting the experiments at room temperature will provide first order evaluation of the ballistic limit, and material debris fragmentation. So, it is a reference test and can be conducted with much simple effort as compared with cooling the target plate. So, if results achieved are good and in according to expectation at room temperature, a progress towards cooling the plate will be conducted, so that it will provide some sort of semi-similar conditions to those prevailing in space environment.

DISCREPENCIES & VALIDATION OF EXPERIMENT

Cross-referencing between other literature reviews that have undertaken similar work has been a key standpoint in making sure the results curated in this report are valid. Within the experiment itself, discrepancy mitigation systems had been put in place to gain reliable results. An oscilloscope was used to verify and corroborate the camera time measurements. For all flat head firings, the impact time measurements from the oscilloscope came within a 5% deviation from the time calculated via the camera. This proves a reliable stream of results obtained for the MBV. For the conical head, oscilloscope readings could not be obtained. The phases shown on the oscilloscope were present only up to 6.25 bar (29.67m/s). Onwards from this pressure, no readings were apparent. The conclusion of this is because of the conical geometry of the harpoon head being too narrow to capture at high velocities. Although, enough validation from the flat heads gave confidence that conical head values were reliable as the same parameters were used between the two harpoons.

The final temperature of the cooled plates was warmer than out the bag, though, before each firing, an infrared thermometer check was taken to make sure temperatures of +/-2°C from -32°C were acquired. The actual temperature was noted each time, and an average was taken which gave this value. Each cooled plate scenario had been timed, from the point of attaining a plate from the bag to the point of firing – and the average time of 90s had a deviation of +/-3s.

To power the propellant within the gas gun chamber, a mechanical knob is used, where the gauge indicates the bars via a needle. The judgment of what pressure the system is at, is based on the human present. There was not a digital system for the gauge present. Changes in velocities are susceptible from one firing to the next because of this, though, in the results, all but one anomaly expressed in graph (a) *Figure 6,* showed consistent results. In this case, the anomaly further enhanced the point being made. Induced drag has been neglected in calculations in this case, as the distance between nozzle and target plate is negligible for the velocities the harpoons are fired at.

CONCLUSION

To mitigate space debris, an ADR space-tether system seems a viable option in the market at current TRLs. The aim of the project was to develop harpoon projectiles that can offer maximum perforation, with minimal obliteration, through the lowest velocity. Two distinct designs in the shape of a flat and conical head are of great interest and a gas gun is used to conduct firings. Aluminum plates are primarily used as targets. Lower MBVs indicate a more efficient system, where less propellant boasts economic advantages. Mass is an integral factor when considering a lower MBV. Mechanical and physical properties of both Al plates and harpoon head material, as well as the energy difference, have a major effect on MBV and perforation results. The nature of perforation from both flat and conical heads is a substantial factor in design, where flat heads result in 'punches'' of material through the plate, whilst conical heads offer a ‘petaling’ feature due to their piercing profile. The perforation features are significant when considering minimum fragmentation in space/vacuum conditions to mitigate further developments of space debris or activation of the Kessler syndrome. Colder climates offer higher tensile and yield strengths for the aluminium plates, where it is concluded these plates require a higher MBV to perforate the Al plate, although, they present flusher perforations. Ambiguity in the reliability of results can be reduced through validation methods such as using an oscilloscope with a high-speed camera.

Though this was not achieved for all the set of the data due to certain limitation of the experimental apparatus.

A new MBV of 49.54m/s has been achieved through this experiment, with 3mm Al plates, compared with JAXAs experiment. For the niche of the flat and conical head designs for tips for space-tethers, progress has been made within this experiment, which can facilitate a foundation for future work.

References

Aalco Metals. (2022). *Aluminium alloy - commercial alloy - 5005 - H34 sheet 5005*. Retrieved 25 September 2022, from https://www.aalco.co.uk/datasheets/Aluminium-Alloy-5005-H34-Sheet_137.ashx

ARES. (n.d.). *LEGEND: 3D/OD evolutionary model*. Retrieved 25 September 2022, from https://orbitaldebris.jsc.nasa.gov/modeling/legend.html

Britannica. (n.d.). Space debris. *Encyclopaedia Britannica*. Retrieved 25 September 2022, from https://www.britannica.com/technology/space-debris

Dudziak, R., Tuttle, S., & Barraclough, S. (2015, August). Harpoon technology development for the active removal of space debris. *Advances in Space Research*, *56*(3), 509–527. https://doi.org/10.1016/j.asr.2015.04.012

How many satellites are orbiting Earth? (2021, September 22). *Astronomy.Com*. Retrieved 25 September 2022, from https://astronomy.com/news/2021/09/how-many-satellites-are-orbiting-earth

Kpenyigba, K., Jankowiak, T., Rusinek, A., Pesci, R., & Wang, B. (2015, May). Effect of projectile nose shape on ballistic resistance of interstitial-free steel sheets. *International Journal of Impact Engineering*, *79*, 83–94. https://doi.org/10.1016/j.ijimpeng.2014.10.007

Mark, C. P., & Kamath, S. (2019, February). Review of active space debris removal methods. *Space Policy*, *47*, 194–206. https://doi.org/10.1016/j.spacepol.2018.12.005

Mataki, T., Akahoshi, Y., Koura, T., Kitazawa, Y., Shimamura, K., Izumiyama, T., Hashimoto, K., Kawamoto, S., Aoyama, J. I., & Fukuta, T. (2016). Evaluation of harpoon tips for debris capture. *TRANSACTIONS OF THE JAPAN SOCIETY FOR AERONAUTICAL AND SPACE SCIENCES, AEROSPACE TECHNOLOGY JAPAN*, *14*(ists30), Pr_33-Pr_37. https://doi.org/10.2322/tastj.14.pr_33

MatWeb. (n.d.a). *Material property data*. Retrieved 25 September 2022, from https://www.matweb.com/search/QuickText.aspx?SearchText=Aluminum%205005

MatWeb. (n.d.b). *Material property data*. Retrieved 25 September 2022, from https://www.matweb.com/search/QuickText.aspx?SearchText=S45C%20Steel

NASA. (2022). *NSSDCA - spacecraft - details*. Retrieved 25 September 2022, from https://nssdc.gsfc.nasa.gov/nmc/spacecraft/display.action?id=1957-001B#:%7E:text=The%20Sputnik%201%20spacecraft%20was,of%20the%20former%20Soviet%20Union

National Space Centre. (2021, January 28). *The Kessler Syndrome*. Retrieved 25 September 2022, from https://spacecentre.co.uk/blog-post/the-kessler-syndrome/

Roth, C. C., Fras, T., & Mohr, D. (2020, October). Dynamic perforation of lightweight armor: Temperature-dependent plasticity and fracture of aluminum 7020-T6. *Mechanics of Materials*, *149*, 103537. https://doi.org/10.1016/j.mechmat.2020.103537

Shen, S., Jin, X., & Hao, C. (2014, August). Cleaning space debris with a space-based laser system. *Chinese Journal of Aeronautics*, *27*(4), 805–811. https://doi.org/10.1016/j.cja.2014.05.002

Smith Metal. (2020a). *1050A Aluminium*. Retrieved 25 September 2022, from https://www.smithmetal.com/1050a.htm

Smith Metal. (2020b). *2024 Aluminium Alloy*. Retrieved 25 September 2022, from https://www.smithmetal.com/2024.htm

Smith Metal. (2020c). *6082 Aluminium*. Retrieved 25 September 2022, from https://www.smithmetal.com/6082.htm

University of Surrey. (2013). *Space Centre pioneers 'gossamer sail' for deorbiting satellites*. Retrieved 25 September 2022, from https://www.surrey.ac.uk/features/surrey-space-centre-pioneers-%E2%80%98gossamer-sail%E2%80%99-deorbiting-satellites